

Magnetotransport in Manganites and the Role of Quantal Phases: Theory and Experiment

S. H. Chun,* M. B. Salamon, Y. Lyanda-Geller, P. M. Goldbart, and P. D. Han

Department of Physics and Materials Research Laboratory, University of Illinois at Urbana-Champaign,
Urbana, Illinois 61801-3080

(Received 20 April 1999)

While low-temperature Hall resistivity ρ_{xy} of $\text{La}_{2/3}(\text{Ca,Pb})_{1/3}\text{MnO}_3$ single crystals can be separated into ordinary (OHE) and anomalous (AHE) contributions, no such decomposition is possible near the Curie temperature T_c . Rather, the ρ_{xy} data collapse to a single function of the reduced magnetization $m = M/M_{\text{sat}}$, with an extremum at $\approx 0.4m$. A new mechanism for the AHE in the inelastic hopping regime is identified that reproduces the scaling curve. An extension of Holstein's model for the hopping OHE, the mechanism arises from the combined effects of the double-exchange-induced quantal phase in triads of Mn ions and spin-orbit interactions.

PACS numbers: 75.30.Vn, 72.20.My, 71.38.+i

Along with the so-called colossal magnetoresistance (CMR) effect, doped perovskite manganites exhibit dramatic variations in the Hall resistivity ρ_{xy} [1–6] near the metal-insulator transition at T_c . In the metallic, low temperature regime, the Hall effect can be reconciled with a positive ordinary Hall effect (OHE) and an anomalous Hall effect (AHE) of opposite sign [5]. However, near T_c , all signatures of the metallic OHE are lost, and the Hall effect becomes a double-valued function of applied field H . In the same region, the longitudinal resistivity ρ_{xx} exceeds the Mott limit, and is better described by hopping conduction. The study of the OHE in the hopping regime has a long history beginning with the work of Holstein [7], who realized that the OHE in hopping conductors requires considering *at least triads* of sites and the attendant Aharonov-Bohm (AB) fluxes through polygons with vertices on those sites. However, how to average over all triads and conducting network structure in disordered systems remains controversial [8,9].

In this Letter, we present new Hall resistivity data on optimally doped manganite single crystals, with emphasis on the regime close to T_c . We demonstrate that the ρ_{xy} data collapse to a single curve when plotted as a function of reduced magnetization. Moreover, we show for the first time that the quantal phase accumulated by hopping charge carriers, a result of the strong-Hund's-rule requirement that outer-shell carriers follow the local configuration of core spins, provides a new AHE mechanism in the inelastic hopping regime. The possibility that Hund's-rule-induced Berry phase [10] contributions can, in the presence of spin-orbit interactions (SOI), lead to AHE in the metallic, band-conductivity regime was first suggested by Kim *et al.* [11]. Here we consider inelastic hopping, relevant to the transition region, and the discrete analog of Berry's phase, appropriately called the Pancharatnam phase [12,13]. By including the effects of SOI, we derive a scaling function for ρ_{xy} that closely follows the collapsed experimental data.

High quality single crystals of $\text{La}_{2/3}(\text{Ca,Pb})_{1/3}\text{MnO}_3$ were grown from 50/50 PbF_2/PbO flux. It was found

that the addition of Ca favors optimally doped crystals; chemical analyses of crystals from the same batch gave the actual composition as $\text{La}_{0.66}(\text{Ca}_{0.33}\text{Pb}_{0.67})_{0.34}\text{MnO}_3$. Specimens for the Hall measurements were cut along crystalline axes from larger, preoriented crystals. Details of the measurement technique and analysis at low T have been presented in [5]. ρ_{xy} and ρ_{xx} were measured simultaneously as functions of H and T . The magnetization of the same sample, measured following the Hall experiment, was used to correct for demagnetization. Figure 1 shows $\rho_{xx}(T)$ at $H = 0, 3,$ and 7 T. Magnetization curves are shown in the inset. The residual resistivity of this sample, $\rho_{xx}^0 \approx 51 \mu\Omega \text{ cm}$, is comparable to the best values obtainable in these materials. The maximum of $d\rho_{xx}/dT$ occurs at 287.5 K and $H = 0$ T, moving to higher T with increasing H . The CMR is 326% at 293 K and 7 T. A

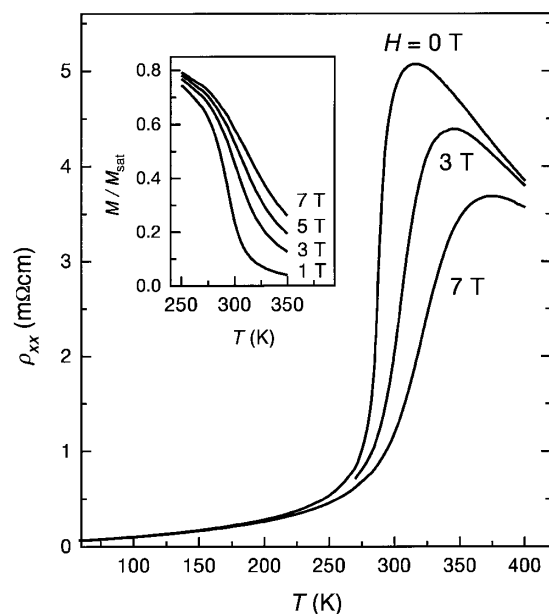


FIG. 1. Main panel: the temperature dependence of $\rho_{xx}(H, T)$ of a $\text{La}_{2/3}(\text{Pb,Ca})_{1/3}\text{MnO}_3$ single crystal at various H . Inset: $M_H(T)$ for the same crystal.

scaling analysis of the magnetization data very close to the metal-insulator transition gives $T_c = 285$ K, but this must be taken cautiously as the scaling exponents differ significantly from those expected from a 3D Heisenberg ferromagnet. Nevertheless, it is clear that ρ_{xx} and M are closely correlated in this system. In ferromagnets, the Hall resistivity is given by [14]

$$\rho_{xy} = R_H B_{in} + R_S \mu_0 M, \quad (1)$$

where R_H is the OHE coefficient; R_S is the AHE coefficient; $B_{in} = \mu_0 H_{app} + \mu_0(1 - N)M$, with N calculated from the sample shape. In Fig. 2, we show ρ_{xy} vs B_{in} at various T . At low T , ρ_{xy} is positive and is linear in B_{in} , indicating that R_S is small. In this metallic regime the OHE arises from the Lorentz force acting on current carriers and the AHE originates from spin-orbit effects (skew scattering and side jumps); see, e.g., [15]. With increasing T , the AHE becomes very large and difficult to analyze near T_c , leading us to seek a different mechanism. An alternative has been proposed [11] for the metallic state, arising from nontrivial spin configurations in manganites, but is not relevant to the transitional region. From Fig. 1, we see that the CMR sets in when ρ_{xx} exceeds 1 m Ω cm. Using a standard Drude-type picture we find that band broadening \hbar/τ at such ρ_{xx} is approximately 0.65 eV, i.e., significantly larger than the bandwidth and the Fermi energy. The resistivity, therefore, exceeds the Mott-Ioffe-Regel limit for metallic conductivity and makes bandlike transport models inappropriate. In contrast, an estimate based on a hopping conductivity model in which localized electrons move between ion sites gives a reasonable estimate of the characteristic attempt frequency of inelastic hopping $W = 3 \times 10^{13} \text{ s}^{-1}$.

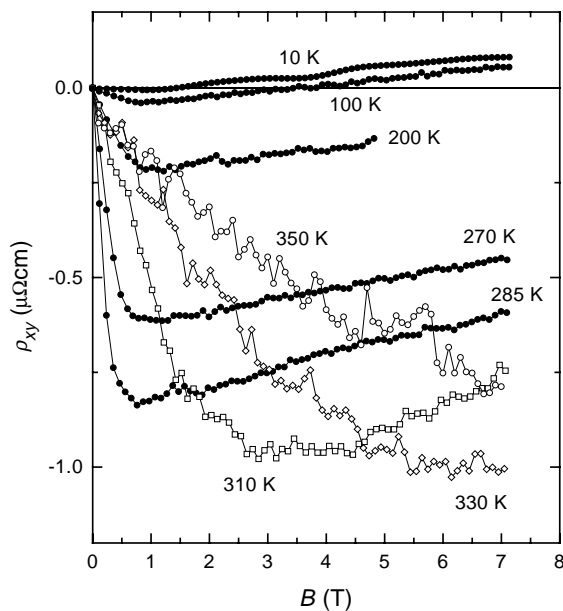


FIG. 2. $\rho_{xy}^T(H)$ of the same crystal at various temperatures.

The picture of localized states in manganites in the vicinity of the transition has been discussed by Varma [16] and Sheng *et al.* [17]. Two types of disorder, intrinsically present in this system, contribute to localization. Magnetic (spin) disorder is Lifshitz type [18] off-diagonal disorder. It is long lived and leads to localized states in the electronic band tail. In addition, the manganites are characterized by substantial static nonmagnetic disorder from the random substitution of La ions by dopant ions. This diagonal, Anderson-type disorder facilitates localization of carriers [17]. We therefore assume that it is reasonable to consider phonon-assisted hopping between localized states as the mechanism of electron transfer in the transitional region [19]. Then ρ_{xx} can be described in terms of Miller-Abrahams resistive network [21,22], in which each resistance of the network is determined by an Anderson-Hasegawa factor in the transfer amplitude $\cos\theta/2$, where θ is the angle between core spins (assumed classical) on a pair of Mn sites [23].

To treat the AHE we require more than a pair of sites and, ignoring any AB fluxes (as we shall not be concerned with OHE), consider spin quantal phases in triads of magnetic ions. These quantal phases are geometric in origin [10]. Indeed, assigning a definite direction \mathbf{n}_i to each core spin-3/2 in the triad, and allowing each outer-shell current carrier a single spin state per site (as required by Hund's rules), we find that a quantal phase

$$\Omega/2 = \tan^{-1} \left[\frac{\mathbf{n}_1 \cdot (\mathbf{n}_2 \times \mathbf{n}_3)}{(1 + \mathbf{n}_1 \cdot \mathbf{n}_2 + \mathbf{n}_2 \cdot \mathbf{n}_3 + \mathbf{n}_3 \cdot \mathbf{n}_1)} \right]$$

arises. This phase controls interference between a direct hop between two sites in the triad and indirect hops between those two sites via the third. Ω is the solid angle of the geodesic triangle on the unit sphere of spin orientations having vertices at $\{\mathbf{n}_1, \mathbf{n}_2, \mathbf{n}_3\}$, and is the quantal analog of the classical optical phase discovered in the context of polarized light by Pancharatnam [12,13,24]. In the hopping regime, the Pancharatnam phase leads to an AHE in an elementary triad with a given set of core-spin orientations in much the same way that an AB flux leads to the OHE in Holstein's spinless model [7].

There is, however, a significant difference between the AHE caused by the Pancharatnam spin phase in triads of magnetic ions and the Holstein OHE resulting from the AB magnetic flux. In the latter case, a uniform applied magnetic field leads to a net macroscopic OHE, even though contributions of triads may partially cancel one another [8]. In the former case (magnetic sites, Pancharatnam flux), if no SOI is taken into account, the presence of macroscopic magnetization of the core spins is insufficient to cause a *macroscopic* AHE. The reason is that we must average over the configurations of the core spins. In the absence of SOI, the distribution of these configurations, although favoring a preferred *direction* (i.e., the magnetization direction $\mathbf{m} \equiv \mathbf{M}/M$), is invariant under a reflection of all core-spin vectors in any plane containing \mathbf{M} while the sign of the quantal phase reverses. This fact, coupled with the

invariance of electron eigenstates under such reflections, guarantees that the macroscopic AHE current will average to zero.

In order to capture the AHE in manganites, we must consider spin-orbit interactions, which lift the reflection invariance of the outer-shell carrier energies and the distribution of core-spin configurations. For a given core-spin configuration, SOI favors one sense of carrier circulation around the triad over the other, and thus favors one sign of the Pancharatnam phase. There are two resulting contributions to the AHE. The first arises from the SOI-generated dependence of eigenenergies of carriers on triads of ions on the three vector products $\mathbf{N}_{jk} \equiv \mathbf{n}_j \times \mathbf{n}_k$ which has Dzyaloshinski-Moriya (DM) form [25]. Such dependence results from the SOI effect on the hopping matrix element t between Mn ions, which is a real number and spin independent in the double-exchange model, but acquires a phase and spin dependence in the presence of SOI. For a hole on a triad [24], $t = t_0(1 + ig\boldsymbol{\sigma} \cdot \mathbf{Q}/Q)$, where t_0 is the matrix element in the absence of SOI, and \mathbf{Q} is the vector area of a triad. When Hund's rule is taken into account, DM terms $\mathbf{N}_{ij} \cdot \mathbf{Q}/Q$ appear in hole eigenenergies. Together with \mathbf{m} , the \mathbf{N}_{jk} yield preferred values for the triad Pontryagin charge $q_P [\equiv \mathbf{n}_1 \cdot (\mathbf{n}_2 \times \mathbf{n}_3)]$ and, hence, a preferred Pancharatnam flux $\sim \mathbf{M} \cdot \mathbf{Q}$. Another contribution arises via a feedback effect in which (fast) carriers provide an effective potential for the (slow) spin system, causing unequal equilibrium probabilities of spin configurations having opposite Pancharatnam fluxes. (Thus, in the first contribution one accounts for SOI in the carrier eigenenergies, which affects the carrier hopping probabilities for a given spin configuration, while in the second the SOI affect only the probability of a given spin configuration.) Thus, q_P and DM terms, acting together, result in a flux of magnetization through the triad $\mathbf{M} \cdot \mathbf{Q}$, giving rise to the AHE in the same way as the AB flux $\mathbf{H} \cdot \mathbf{Q}$ results in the OHE for localized carriers in [7–9].

We assume that transport in the transition region is dominated by hopping processes, giving rise to a longitudinal conductivity $\sigma_{xx} = (ne^2 d^2/k_B T)W_0 \cos^2(\theta/2)$, where d is the distance between ions. Here W_0 is the probability of (single) phonon-assisted direct hops and we have explicitly separated Anderson-Hasegawa factors $\cos^2(\theta/2)$. The AHE conductivity, correspondingly, is given by $\sigma_{xy} = (ne^2 d^2/k_B T)W_1$, where W_1 is the probability of hopping between two ions via an intermediate state on a third ion, and includes Anderson-Hasegawa factors. We now determine the ratio between direct and indirect hopping rates as a function of the spin texture. Because W_1 involves two-phonon processes, we write $W_1/W_0^2 = \alpha \hbar \zeta/k_B T$, where α is a numerical factor describing the multiplicity of the various carrier-phonon interference processes (see [7]), the number of intermediate sites, and the difference between nearest-neighbor and next-nearest-neighbor hopping amplitudes, with ζ as an asymmetry parameter. For the OHE, $\zeta \propto \sin(\mathbf{B} \cdot \mathbf{Q}/\phi_0)$, where \mathbf{Q} is the area vector of the triangle enclosed by the three sites. In the AHE case

$\zeta \approx 3q_P g[\mathbf{Q} \cdot (\mathbf{n}_j \times \mathbf{n}_k)]/4$ [24], where \mathbf{n}_j are unit vectors of the core spins in the triad, and q_P is the volume of a parallelepiped defined by core-spin vectors. The AHE resistivity is given by

$$\rho_{xy} \approx -\sigma_{xy}/\sigma_{xx}^2 = -\frac{1}{ne} \left(\frac{\alpha \hbar \zeta}{ed^2} \frac{1}{\cos^4(\theta/2)} \right). \quad (2)$$

The evaluation of Eq. (2) reduces to a determination of $\cos(\theta/2)$ and products $(\mathbf{n}_j \times \mathbf{n}_k)$ and q_P that survive averaging over triads. In contrast to the hopping OHE in doped semiconductors [8], where only two sites in an optimal OHE triad are connected to the conducting network (CN), all three triad sites must participate in the CN if they are to contribute to the AHE. Our argument is that if one of the sites is not a part of the CN then its core spin must be roughly opposite that of the other two spins, yielding a vanishingly small q_P . It is reasonable then to assume that the CN is formed by ions with splayed core spins oriented roughly in the direction of average magnetization \mathbf{m} . We then consider the square lattice formed by Mn ions in planes perpendicular to \mathbf{m} , and assume that the core spins of the four ions in a typical elementary plaquette belonging to CN lie equally spaced on the cone whose half angle is given by $\beta = \cos^{-1}[M(H, T)/M_{\text{sat}}]$. A typical pair of ions that determines the longitudinal current and a typical triad can now be chosen from ions of this plaquette. From elementary geometry, it follows that $2 \cos^2(\theta/2) = 1 + \cos^2 \beta$, $q_P = 2 \cos \beta \sin^2 \beta$, and $\mathbf{m} \cdot (\mathbf{n}_j \times \mathbf{n}_k) = \sin^2 \beta$. To find the AHE magnitude, we estimate the characteristic values of $|\mathbf{g}| \sim g \sim Ze^2/4m_e c^2 d_0$, where d_0 is the radius of an Mn core d state. An estimate based on free electron parameters is reasonable (see [24]) and gives $g \sim 5 \times 10^{-4}$. Then, the magnitude of the DM term $\sim g t_0 \sim 0.02$ meV, and is much smaller than the magnitude of the Heisenberg exchange term. However, for the AHE in localization regime DM terms are crucial. The magnitude of ρ_{xx} and ρ_{xy} in the regime of abrupt increase of ρ_{xx} depends not only on properties of individual pairs (triads), but also on how they are connected to the CN. In the low temperature limit of our model, where the CN is still fully connected, taking $n = 5.6 \times 10^{21} \text{ cm}^{-3}$, $W_0 \sim 2.5 \times 10^{13} \text{ s}^{-1}$, and $\cos \beta = 0.6$ from the magnetization data at $T = 275$ K (Fig. 1), we obtain $\rho_{xx} \approx 1 \text{ m}\Omega \text{ cm}$ which coincides with the value of the experimentally observed ρ_{xx} (Fig. 1). The AHE contribution to ρ_{xy} , assuming $\alpha = 2.5$, is then $\rho_{xy} = -0.5 \mu\Omega \text{ cm}$, in agreement with the experimentally observed ρ_{xy} at the same T (Fig. 2). The equivalent expression for the hopping OHE has $\zeta \approx \cos^2(\theta/2) \cos \beta \sin(\mathbf{B} \cdot \mathbf{Q}/\phi_0)$ and, at $B = 1$ T, is an order of magnitude smaller than the AHE. We expect the macroscopic hopping AHE and OHE to have the same sign, opposite that of the OHE in the metallic regime.

To relate ρ_{xy} to $m \equiv |\mathbf{m}|$, we introduce a percolation factor P for σ_{xx} describing the connectivity of the pair to the CN; for the AHE conductivity the corresponding factor would be P^2 because both pairs in a triad must, as

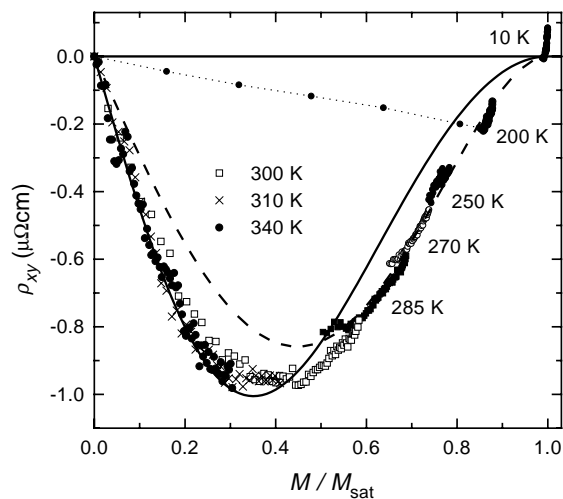


FIG. 3. Scaling behavior between ρ_{xy} and the sample magnetization M . The solid line is a fit to Eq. (3); the dashed line is the numerator of Eq. (3) only. There are no fitting parameters except normalization.

discussed above, belong to the CN. It is remarkable that throughout the localization regime, ρ_{xy} is, nevertheless, determined by currents formed in individual pairs and triads, because the factors of P cancel. Therefore, as long as qP and the angles between neighboring spins can be directly related to $m \equiv M/M_{\text{sat}} = \cos\beta$, ρ_{xy} depends on H and T only through $m(H, T)$, and is given by

$$\rho_{xy} = \rho_{xy}^0 m(1 - m^2)^2 / (1 + m^2)^2. \quad (3)$$

The corresponding curve is shown in Fig. 3, where the data of Fig. 2 are replotted as a function of M/M_{sat} . At and above T_c the data fall on a smooth curve that reaches an extremum at $M/M_{\text{sat}} \approx 0.4$. Below T_c the data first change rapidly with M as domains are swept from the sample before saturating and following the general trend. At the lowest temperatures, the metallic OHE appears as a positive contribution at constant magnetization. The solid curve in Fig. 3 follows Eq. (3) with $\rho_{xy}^0 = -4.7 \mu\Omega \text{ cm}$, consistent with the estimates of ρ_{xx} and ρ_{xy} given above. Down to 285 K, which is the T_c determined by the scaling analysis, Eq. (2) describes the data reasonably well. In addition, the extremum is located at $M/M_{\text{sat}} = \cos\beta \approx 0.35$, close to the experimental extremum. Below T_c , ρ_{xx} is metallic and no longer dominated by magnetic disorder. However, local spin arrangements are still manifested in the AHE, e.g., via asymmetric scattering. Then the numerator of Eq. (3), $m(1 - m^2)^2$, is essentially the behavior of σ_{xy} alone and has an extremum at $m = 1/\sqrt{5} = 0.45$ as shown by the dashed line in Fig. 3. The broader maximum in the data suggests a shift toward a hopping model for ρ_{xx} and ρ_{xy} as the sample is warmed through the metal-insulator transition.

In conclusion, we find that the Hall resistivity of a $\text{La}_{2/3}(\text{Ca,Pb})_{1/3}\text{MnO}_3$ single crystal is solely determined by the sample magnetization near and somewhat above the transition temperature. A model for the AHE, based

on the Holstein picture in which interference between direct inelastic hops and those via a third site is sensitive to the quantal phase, explains the results quite well. Unlike the Holstein Hall effect in the presence of Aharonov-Bohm flux, the anomalous Hall effect stems from quantal phase due to the strong-Hund's-rule coupling that forces the hopping charge carrier to follow the local spin texture, and from spin-orbit interactions. It is the strength of the Hund's coupling that enables effects due to quantal spin phases to persist at and above room temperature. Below T_c , the AHE competes with the OHE as long-range magnetic order, and presumably an infinite percolating cluster and metallic conductivity develop.

This work was supported in part by DOE DEFG-91ER45439 through the Illinois Materials Research Laboratory.

*Present address: Department of Physics, The Pennsylvania State University, University Park, PA 16802.

- [1] G. J. Snyder *et al.*, Appl. Phys. Lett. **69**, 4254 (1996).
- [2] M. Jaime *et al.*, Phys. Rev. Lett. **78**, 951 (1997).
- [3] P. Matl *et al.*, Phys. Rev. B **57**, 10248 (1998).
- [4] A. Asamitsu and Y. Tokura, Phys. Rev. B **58**, 47 (1998).
- [5] S. H. Chun *et al.*, Phys. Rev. B **59**, 11155 (1999).
- [6] S. H. Chun *et al.* (in preparation).
- [7] T. Holstein, Phys. Rev. **124**, 1329 (1961); D. Emin and T. Holstein, Ann. Phys. (N.Y.) **53**, 439 (1969).
- [8] Y. M. Galperin *et al.*, Sov. Phys. JETP **72**, 193 (1991).
- [9] O. Entin-Wohlman *et al.*, Phys. Rev. Lett. **75**, 4094 (1995).
- [10] N. Nagaosa and P. A. Lee, Phys. Rev. Lett. **64**, 2450 (1990); E. Müller-Hartmann and E. Dagotto, Phys. Rev. B **54**, 6819 (1996).
- [11] Y. B. Kim *et al.*, cond-mat/9803350. This preprint was superseded by J. Ye *et al.*, Phys. Rev. Lett. **83**, 3737 (1999).
- [12] S. Pancharatnam, Proc. Indian Acad. Sci. A **44**, 247 (1956).
- [13] M. V. Berry, Int. J. Mod. Opt. **34**, 1401 (1987).
- [14] C. M. Hurd, *The Hall Effect in Metals and Alloys* (Plenum Press, New York, 1972).
- [15] J. Luttinger, Phys. Rev. **112**, 739 (1958); P. Nozières and C. Lewiner, J. Phys. (Paris) **34**, 901 (1973).
- [16] C. M. Varma, Phys. Rev. B **54**, 7328 (1996).
- [17] L. Sheng *et al.*, Phys. Rev. Lett. **79**, 1710 (1997).
- [18] I. M. Lifshitz, Sov. Phys. Usp. **7**, 549 (1964).
- [19] Recent data [6] indicate that polarons [20] can play some role in $\text{La}_{2/3}(\text{Ca,Pb})_{1/3}\text{MnO}_3$ and similar compounds only significantly above T_c .
- [20] A. J. Millis, P. B. Littlewood, and B. I. Shraiman, Phys. Rev. Lett. **74**, 5144 (1995).
- [21] V. Ambegaokar *et al.*, Phys. Rev. B **4**, 2612 (1971).
- [22] A. Efros and B. Shklovskii, *Electronic Properties of Disordered Conductors* (Springer, New York, 1984).
- [23] C. Zener, Phys. Rev. B **82**, 403 (1951); P. W. Anderson and H. Hasegawa, Phys. Rev. **100**, 675 (1955).
- [24] Y. Lyanda-Geller *et al.*, cond-mat/9904331.
- [25] I. E. Dzyaloshinski, J. Phys. Chem. Solids, **4**, 241 (1958); T. Moriya, Phys. Rev. Lett. **4**, 5 (1960). For bandlike electrons terms of similar type were discussed in P. M. Levy and A. Fert, Phys. Rev. B **23**, 4667 (1981).